Dissociation Energy and Long-Range Potential of Diatomic Molecules from Vibrational Spacings of Higher Levels*

ROBERT J. LEROY AND RICHARD B. BERNSTEIN

Theoretical Chemistry Institute and Chemistry Department, University of Wisconsin, Madison, Wisconsin 53706

(Received 12 December 1969)

An expression is derived which relates the distribution of vibrational levels near the dissociation limit D of a given diatomic species to the nature of the long-range interatomic potential, in the region where the latter may be approximated by $D-C_n/R^n$. Fitting experimental energies directly to this relationship yields values of D, n, and C_n. This procedure requires a knowledge of the relative energies and relative vibrational numbering for at least four rotationless levels lying near the dissociation limit. However, it requires no information on the rotational constants or on the number and energies of the deeply bound levels. D can be evaluated with a much smaller uncertainty than heretofore obtainable from Birge–Sponer extrapolations. The formula predicts the energies of all vibrational levels lying above the highest one measured, with uncertainties no larger than that of the binding energy of the highest level. The validity of the method is tested with model potentials, and its usefulness is demonstrated by application to the precise data of Douglas, Møller, and Stoicheff for the $B\,^3\Pi_{0u}{}^+$ state of Cl_2.

I. INTRODUCTION

For more than four decades the Birge–Sponer[1] extrapolation procedure has been employed, with only minor modifications,[2,3] for the determination of values for dissociation limits of diatomic molecules from experimental vibrational spacings $\Delta G_{v+1/2}$.[4] One of the great virtues of this method is its simplicity, as exemplified by the exact linear relationship between $\Delta G_{v+1/2}$ and v for a Morse potential. In this case, $\Delta G(v)$ [5] extrapolates to zero at $v_D=[(\omega_e/2\omega_e x_e)-\frac{1}{2}]$, where v_D is the noninteger "effective" vibrational index of the dissociation limit.[4] For more realistic potentials it is well known that the Birge–Sponer (B–S) plot shows positive curvature in the region just prior to dissociation, due to the dominating influence of the long-range "tail" of the interatomic potential.[2–4,6] Graphical extrapolation to the dissociation limit is therefore less reliable, and uncertainties of several cm^{-1} are common in values so obtained for the dissociation limit D.

The WKB-based method to be described takes advantage of the dominating influence of the long-range portion of the potential on the uppermost vibrational levels. It requires only the energies and relative vibrational numbering of four or more rotationless levels lying close to the dissociation limit D (i.e., less than $\approx 10\%$ of the well depth below D). These are fitted to an analytical approximation formula, yielding "best" estimates of D and of the long-range interatomic potential. Although a proper RKR analysis yields a much more accurate estimate of the potential,[7] it is much more restrictive than the present method since it requires as additional information the energies and B_v constants of *all* levels below the one whose turning points are being calculated. Furthermore, the RKR approach provides no estimate of D or of the energies or even of the total number of vibrational levels above the highest one observed, and offers no direct means of extrapolating beyond the observed levels.

II. METHOD

A. Derivation

The starting point of the present treatment is the first-order WKB quantum condition for the eigenvalues of a potential $V(R)$:

$$v+\tfrac{1}{2}=\frac{(2\mu)^{1/2}}{\pi\hbar}\int_{R_1(v)}^{R_2(v)}[E(v)-V(R)]^{1/2}dR, \quad (1)$$

where $E(v)$ is the energy of level v and $R_1(v)$ and $R_2(v)$ are its classical turning points: $E(v)=V[R_1(v)]=V[R_2(v)]$. Although the allowed eigenvalues correspond to integer v, it is convenient to treat v as a continuous variable.

Differentiation of Eq. (1) with respect to $E(v)$ yields

$$\frac{dv}{dE(v)}=(\pi\hbar)^{-1}(\tfrac{1}{2}\mu)^{1/2}\int_{R_1(v)}^{R_2(v)}[E(v)-V(R)]^{-1/2}dR. \quad (2)$$

Consideration of the nature of the integrand in Eq. (2) suggests that the integral will be very nearly unchanged if the exact $V(R)$ is replaced by an approximate function which is accurate near the outer turning point $R_2(v)$. This is illustrated in Fig. 1 for the case of a model potential, chosen to be of the Lennard-Jones (12,6) form.[8] Using the asymptotic approximation for $V(R)$,

$$V(R)=D-C_n/R^n, \quad (3a)$$

where D is the dissociation limit of the potential, C_n is given by

$$E(v)=D-C_n/[R_2(v)]^n. \quad (3b)$$

Changing the variable of integration to $y\equiv R_2(v)/R$, Eq. (2) becomes

$$\frac{dv}{dE(v)}=(\pi\hbar)^{-1}(\tfrac{1}{2}\mu)^{1/2}\frac{C_n{}^{1/n}}{[D-E(v)]^{1/2+1/n}}\times\int_1^{R_2/R_1}y^{-2}(y^n-1)^{-1/2}dy.$$

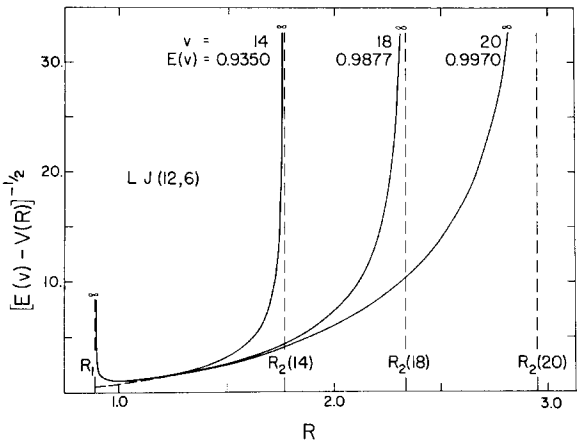

FIG. 1. Exact integrand (solid curves) of Eq. (2) for three levels of a "standard" 24-level LJ (12,6) potential.[8] The dashed segment of curve near R_1 is the approximate integrand $[E(v)-(1-2/R^6)]^{-1/2}$ for $v=20$. The dashed vertical lines are the turning points, where the exact integrand is singular.

In the limit $R_1(v)\to 0$ [i.e., $R_2(v)/R_1(v)\to\infty$] this integral is well known.[9] This yields an approximate analytical expression for $dE(v)/dv$ near the dissociation limit:

$$\frac{dE(v)}{dv}=\hbar\left(\frac{2\pi}{\mu}\right)^{1/2}\frac{\Gamma(1+1/n)}{\Gamma(\frac{1}{2}+1/n)}\frac{n}{C_n^{1/n}}[D-E(v)]^{[(n+2)/2n]}$$
$$=K_n[D-E(v)]^{[(n+2)/2n]}, \quad (4)$$

where K_n is an obvious collection of constants and $\Gamma(x)$ is the gamma function.[10] Note that $dE(v)/dv$ is closely related to the conventional Birge–Sponer ordinate[5]; cgs units are used throughout.

Equation (4) shows that for the uppermost vibrational levels of a given diatomic species, the spacings depend only upon the long-range potential parameters D, n, and C_n. Thus, for electronic states with the same long-range potential, B–S plots for levels near D will be precisely superimposable upon shifting of their abscissa (v) scales. This result is discussed further in Appendix A.

For sets of vibrational levels which can be described by Eq. (4), the curvature of the B–S plot must be positive since[5]

$$d^3E(v)/dv^3=[(n+2)/n^2]K_n^3[D-E(v)]^{3/n-1/2}$$
$$=d^2\Delta G(v)/dv^2$$
$$\cong\tfrac{1}{2}[d^2(\Delta G_{v-1/2}+\Delta G_{v+1/2})/dv^2]. \quad (5)$$

For $n=6$, this curvature is a constant; for $n>6$, it increases with increasing v, becoming infinite at the dissociation limit; for $n<6$, it decreases to zero at D. Positive curvature of a B–S plot for a set of experimental vibrational energies is therefore a necessary (though not sufficient) condition for the applicability of the present method.

In practical applications it is most convenient to employ the integrated form of Eq. (4),[11] which for $n\neq 2$ is

$$E(v)=D-[(v_D-v)H_n]^{[2n/(n-2)]}, \quad (6)$$

where $H_n=[(n-2)/2n]K_n$ and v_D is an integration constant.[12,13] For $n>2$, v_D takes on physical significance as the effective (noninteger) vibrational index at the dissociation limit, provided that the potential is well approximated by Eq. (3) from the highest observed levels up to D. In this case, truncation of v_D to an integer yields the vibrational index of the uppermost rotationless level, say N_D. It is interesting to note that the "natural" dependent and independent variables in Eq. (6) are, respectively, the binding energy $D-E(v)$ and the vibrational "index" counted down from D (for $n>2$). Applications of the present method are based upon the fitting of experimental energies $E(v)$ to Eq. (6) to yield values of the four quantities D, n, C_n, and v_D. This is discussed further in Secs. II.D and III.

B. Special Cases

While the potentials considered above ($n>2$) are of most practical interest, results for $n<2$ will be noted. Here the integration constant v_D must be *smaller* than any of the v values of the levels being fitted (and may even be negative) since K_n is positive and $(n-2)$ is negative [see Eq. (6)]. For $n=1$, Eq. (6) becomes

$$D-E(v)=(\mu/2\hbar^2)C_1^2/(v-v_D)^2,$$

which is the exact quantum result for a pure R^{-1} potential if one sets $v_D=-1$.[14] For $n=2$, integration of Eq. (4) yields

$$D-E(v)=[D-E(0)]\exp[-\pi\hbar v(2/\mu C_2)^{1/2}]. \quad (7)$$

Here the assignment of any given level as $v=0$ is arbitrary since the levels cannot be enumerated either down from D or up from a lowest level.[15] Equation (7) is identical to the exact quantal result[14] except that it omits the (usually small) effect on the apparent C_2 constant of the Langer correction[16] to the WKB integral, Eq. (1).

The present approach can also be applied to potentials whose long-range tails are not of the inverse-power form. For example, consider any potential with an attractive exponential tail,[17] such that at large R, $V(R)=D-Ae^{-\beta R}$. Applying the same approximations [replacing the full potential in Eq. (2) by its tail and letting $R_1\to 0$], an expression analogous to Eq. (4) is obtained:

$$\frac{dE(v)}{dv}=\frac{(2/\mu)^{1/2}\hbar\beta[D-E(v)]^{1/2}}{1-(2/\pi)\sin^{-1}\{[D-E(v)]/A\}^{1/2}}. \quad (8)$$

As with Eq. (4), in this case the vibrational spacings near D depend only on the potential parameters (here D, β, and A), and to a first approximation (ignoring the arcsin term) they are independent of A. Integra-

tion of this expression yields

$$\left(\frac{D-E(v)}{A}\right)^{1/2}\left[1-\frac{2}{\pi}\sin^{-1}\left(\frac{D-E(v)}{A}\right)^{1/2}\right]$$
$$+\frac{2}{\pi}\left[1-\left(1-\frac{D-E(v)}{A}\right)^{1/2}\right]=\frac{\hbar\beta}{(2\mu A)^{1/2}}(v_D-v),$$

where the integration constant v_D has the same physical significance as in the inverse power ($n>2$) case. Upon expanding the left-hand side as a power series in $\{[D-E(v)]/A\}^{1/2}$, reversion of the series yields

$$D-E(v)=(\hbar^2\beta^2/2\mu)(v_D-v)^2[1+(v_D-v)Y$$
$$+\tfrac{5}{4}(v_D-v)^2Y^2+\cdots], \quad (9)$$

where

$$Y=(2/\mu A)^{1/2}\hbar\beta/\pi. \quad (10)$$

As with the inverse-power potential, the B–S plot will show positive curvature; however here the curvature is quite small, and to first order (setting $Y=0$) it is zero.[18]

This result [Eq. (9)] for potentials with an exponential tail is particularly useful since it allows a test of the approximations underlying the present treatment. One may compare Eq. (9) with the exact quantal results for one realistic model potential with an exponential tail, the Morse potential[19]: $V_M(R)=D_e\{1-\exp[-\beta(R-R_e)]\}^2$, whose eigenvalues are given by[4,14]

$$D-E(v)=(\hbar^2\beta^2/2\mu)(v_D-v)^2=\omega_e x_e(v_D-v)^2, \quad (11)$$

where v_D is, as before, the effective vibrational index at D. Clearly, in the limit $Y\to 0$, the distribution of vibrational levels predicted by Eq. (11) agrees with that of Eq. (9). This is true despite the different v_D's, which merely correspond to a change in vibrational numbering and a small shift in the eigenvalues (arising from the small change in v_D-N_D). In effect, this merely shifts the abscissa scale in the B–S plot. The influence of the short-range portion of the Morse potential is thus merely to remove the small "correction" terms in $(v_D-v)Y$ from Eq. (9), yielding Eq. (11). The value of Y depends on both β and the coefficient of the long-range (attractive) exponential term in $V_M(R)$, $A=2D_e\exp(\beta R_e)$. Substituting the latter into Eq. (10) and using known relations among the Morse parameters,[4] one identifies

$$Y=(8^{1/2}/\pi)(\omega_e x_e/\omega_e)\exp(-\tfrac{1}{2}\beta R_e), \quad (12)$$

which shows that for typical diatomics $Y\ll 1$.

C. Significance of Parameters and Sources of Error

Perturbation theory suggests[20] that near the dissociation limit, the internuclear interaction may be expressed as a sum of inverse (integer) power terms in R:

$$V(R)=D-\sum_m C_m/R^m. \quad (13)$$

Over any small interval, Eq. (3a) is a close approximation to Eq. (13), if one considers n to be an "effective" or "local" power which corresponds to a weighted average of the different m values,[21] e.g.,

$$n=\frac{\sum_m (m+1)mC_m/[R_2(v)]^{m+1}}{\sum_m mC_m/[R_2(v)]^{m+1}}-1. \quad (14)$$

In the limit $v\to v_D$, as $R_2(v)$ reaches the asymptotic region, the effective noninteger power $n\to\tilde{n}$, the (integer) smallest power contribution to Eq. (13). As long as the potential for the state in question is well behaved,[22] fits of Eq. (6) to different subsets of a given energy spectrum should all yield essentially the same value of D, though the "local" values of n, C_n, and v_D differ slightly.

At somewhat shorter separations, exponential-type exchange forces replace the inverse-power terms in dominating the interaction[20]; thus, the B–S plot becomes increasingly linear for the deeper levels.[18] However, the approximations of the present treatment are worse for these more deeply bound levels, so only the region dominated by the long-range inverse-power terms (positive curvature of the B–S plot) should be treated by the present method.

There are two main sources of error inherent in the approximations represented by Eq. (3). First and most obvious is the neglect of the singularity at $R_1(v)$ in the exact integrand of Eq. (2) (see Fig. 1). This omission tends to make the estimate of the integral used to obtain Eq. (4) somewhat small, and since the relative magnitude of this error decreases for the higher levels, the effect will be to yield values of both n and C_n which are somewhat too large.

The second source of error arises from the fact that a realistic long-range interatomic potential is a sum of attractive inverse-power terms [see Eq. (13)], in contrast to the single attractive term in the model LJ (12,6) potential. This means that whatever the effective inverse-power precisely at a given $R_2(v)$ [from Eq. (14)], terms with higher powers contribute relatively more to the potential for $R<R_2(v)$, so that the exact integrand of Eq. (2) is smaller than that for the single C_n/R^n function which best fits the potential at $R_2(v)$. This error has the opposite effect of the first, tending to produce values of n and C_n which are slightly too small. The former error is most serious for the deeper levels, while the latter dominates the situation as n [see Eq. (14)] approaches its asymptotic value $\tilde{n}$.[23]

A third potential source of error arises from use of the first-order WKB approximation [given by Eq. (1)], compounded by the omission of the Langer correction.[16] However the effect of this approximation is expected to be negligible.[24]

Values of D, n, and C_n obtained on fitting any given set of vibrational energies to Eq. (6) yield a "local" estimate of the potential in the form of Eq. (3). Be-

cause of the errors described above, this estimate of the potential will be somewhat too deep when using data for the deeper levels and slightly too shallow when considering only the highest levels. This is illustrated by the examples considered in Sec. III.

Next in importance to D are the power $\tilde{n}$ and coefficient C_n of the longest-range ($\tilde{n}$th-power) term in the expansion for the potential [see Eq. (13)]. The errors in n (see above) which induce slight errors in D, may also weaken the accuracy of $\tilde{n}$. However, for many electronic states $\tilde{n}$ is known from theoretical considerations[25]; the only question is whether the levels being fitted lie close enough to the dissociation limit D to be governed mainly by the asymptotic R^{-n} ($n=\tilde{n}$) term of the potential. If this is so, it is desirable to constrain n to be equal to $\tilde{n}$ and employ a three parameter fit to Eq. (6) [or if $\tilde{n}=2$, a two parameter fit to Eq. (7)]. This should yield improved accuracy in D and provide significant values of the theoretically interesting C_n ($n=\tilde{n}$) and v_D.

D. Implementation

In this section, a procedure is described for the practical application of the present method to experimental data in a manner intended to yield the best possible estimates of the parameters D, n, C_n, and (for $n\neq 2$) v_D. The general case of $n\neq 2$ will be considered first, followed by a brief discussion of the situation for $n=2$.

A least-squares fit of experimental energies directly to Eq. (6) is the most general way of obtaining the best values of the four quantities.[26] However, since this expression is nonlinear in the parameters, the general regression problem may have no unique solution since the sum of squares may show local minima which do not correspond to the best parameter values. This problem can be avoided if the initial trial parameter values (required by nonlinear regression procedures) are sufficiently accurate. The necessary trial values for n and v_D may be obtained from a fit to a linear expression obtained on combining derivatives from Eq. (6)[27]:

$$E'(v)/E''(v) = -[(n-2)/(n+2)](v_D-v). \quad (15)$$

Holding fixed the n and v_D values thus obtained, Eq. (6) becomes linear in a new independent variable, $w\equiv\{[(n-2)/2n](v_D-v)\}^{[2n/(n-2)]}$:

$$E(v) = D - wK_n^{[2n/(n-2)]}. \quad (16)$$

This yields trial values of D and K_n [which gives C_n via Eq. (4)]. The four parameter values thus obtained are good starting approximations for the direct nonlinear fit of the experimental energies to Eq. (6)[28]; the linearity of Eqs. (15) and (16) makes this approach particularly straightforward.[29,30]

While Eq. (16) may be used only for $n\neq 2$, Eq. (15) is also valid for $n=2$ since combining the derivatives of Eq. (7) shows that

$$E'(v)/E''(v) = -(\pi\hbar)^{-1}(\tfrac{1}{2}\mu C_2)^{1/2}.$$

Thus, even though $v_D(n=2)=\infty$,

$$\lim_{n\to 2}[(n-2)/(n+2)]v_D(n) = (\pi\hbar)^{-1}(\tfrac{1}{2}\mu C_2)^{1/2}.$$

Manipulating Eq. (4) and its derivatives, one obtains simple expressions yielding trial values of D and C_n:

$$D = E(v) - [(n+2)/2n][E'(v)]^2/E''(v) \quad (17a)$$

and

$$K_n = E'(v)/[D-E(v)]^{[(n+2)/2n]}, \quad (17b)$$

where, as before, C_n is obtained from K_n. While Eqs. (17) are valid for all n, in practice they are somewhat less accurate and more difficult to use than is Eq. (16).[31]

III. APPLICATIONS

A. Dissociation Limit and Potential Tail from Eigenvalues of a Model Potential

The method is first applied to the exact eigenvalues of the previously mentioned (Sec. II.A) 24-level LJ (12,6) potential[8]: $V(R)=1+1/R^{12}-2/R^6$ (here $D=1$, $\tilde{n}=6$, $C_6=2$). A B–S plot of the eigenvalues of any LJ (12,6) potential has positive curvature everywhere.[6] However, as discussed in Sec. II, consideration of the deeper levels by the present method is inappropriate, so the following analysis deals only with the eleven levels lying less than 10% of the well depth below the dissociation limit [i.e., $D-E(v)\leq 0.1D_e$].[19] Throughout this section, energies are expressed in units of the well depth (i.e., set $D_e=1$), length in units of the equilibrium distance (i.e., set $R_e=1$), and the zero of energy is set at the potential minimum.

The calculated eigenvalues[8] for the eleven highest levels were smoothed by fitting them to a 5th order polynomial in v, in order to obtain the derivatives on

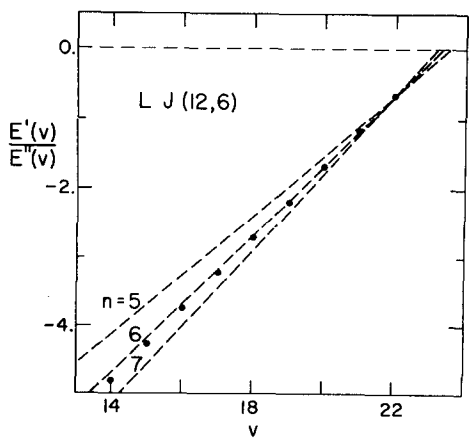

FIG. 2. $E'(v)/E''(v)$ vs v for the highest levels of the 24-level LJ (12,6) potential.[32] The broken lines have slopes corresponding to integer $n=5$, 6, and 7 [see Eq. (15)].

the left-hand side of Eq. (15). Figure 2 shows a plot of this derivative ratio vs v, compared with lines whose slopes correspond [via Eq. (15)] to integer $n=5$, 6, and 7.[32] A least-squares fit of these derivative ratios to Eq. (15) yielded $n=6.29$ and $v_D=23.27$ [32]; fixing n and v_D at these values, a subsequent fit of the eigenvalues to Eq. (16) yielded $D=1.0-1.31\times10^{-5}$ (the correct value is exactly 1.0) and $C_n=3.43$. These estimates of the parameters were then used as the initial trial values for a nonlinear fitting of the eleven energies to Eq. (6).[26,29] The parameters thus obtained were $D=1.0-1.29\times10^{-5}$, $n=6.30$, $C_n=3.46$, and $v_D=23.25$.

The above fitting procedure was then repeated several times while the deeper levels were successively omitted. Levels in the interval $v_L\leq v\leq v_H$ were included in a given fit; v_H was fixed at 23 (the highest level) while v_L was successively increased from 13 to 19.[33] In Fig. 3 the resulting parameter values (solid curves) are plotted against the energy of the lowest level included in a given fit, $E(v_L)$.

For a LJ (12,6) potential $\tilde{n}=6$, and the effective n at the outer turning point [from Eq. (14)] is always less than six. Thus the fact that four-parameter fits to Eq. (6)[29] always yield $n>6$ must be due to the first

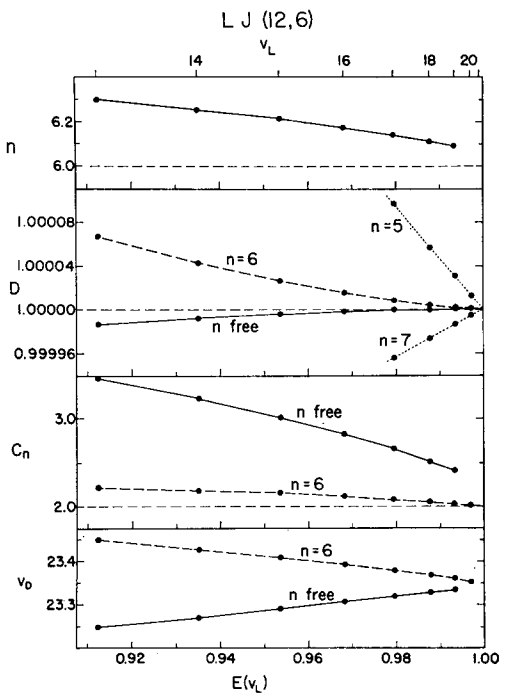

FIG. 3. Results of fitting Eq. (6) to the vibrational levels of the 24-level LJ (12,6) potential.[8,26,29] The points correspond to fits of levels v_L up to $v_H=23$. The broken horizontal lines denote the exact quantities $\tilde{n}=6$, $D=1.0$, and $C_6=2.0$. The "best" $n=6$ estimate of v_D is 23.353, in good agreement with the value 23.358 generated from the analytic expression of Stogryn and Hirschfelder.[36] Points joined by solid lines correspond to four-parameter fits with n being varied freely, while the others correspond to three-parameter fits with n held fixed at the indicated values. (*Note added in proof*: The extension of the dotted curves for D beyond $V_L=20$ was unintended.)

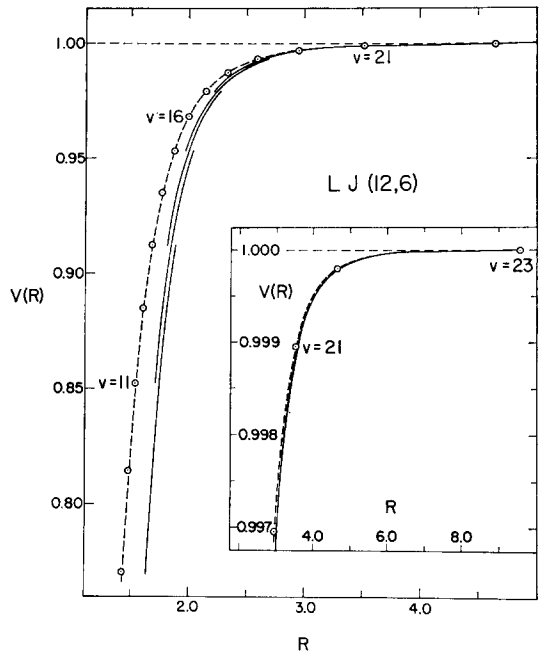

FIG. 4. Piecewise potentials constructed from three-parameter fits (D constrained at 1.0) of the LJ (12,6) vibrational energies[8] to Eq. (6).[26,29] ⊙, exact turning points for the specified levels; —, segments obtained from fits; - - -, exact asymptotic R^{-6} potential tail.

type of error discussed in Sec. II.C. To obtain more accurate estimates of D, C_n, and v_D, the above fitting procedure was repeated with n fixed at $\tilde{n}=6$. Levels v_L to $v_H=23$ were fitted while v_L was increased successively from 13 to 20,[29,33] yielding the parameter values joined by the dashed curves in Fig. 3. This procedure was repeated with n fixed in turn at 5 and 7, yielding the dotted curves in Fig. 3. Consideration of the different curves for D suggests that their comparative convergence (flattening) is a test of convergence to the true value of $\tilde{n}$.[34] In general, the three-parameter fits with n fixed at $\tilde{n}$ yield meaningful values of $C_n(n=\tilde{n})$ and v_D and give better estimates of D than do the four-parameter fits. "Best" values of all parameters are obtained from the right-hand ends of the dashed curves in Fig. 3: $D=1.0+0.13\times10^{-5}$, $C_6=2.01$, and $v_D=23.353$. This v_D value agrees well with the first order WKB value of 23.358.[35]

As pointed out above, the dominant error affecting these LJ (12,6) results arises from the effect of the singularity at $R_1(v)$. The values of n and C_n obtained from the four-parameter fits (and the C_6 values from the three-parameter fits) are somewhat large; as expected, the error diminishes as the deeper levels are successively dropped.

As discussed in Sec. II.C, the present method yields values of D, n, and C_n which provide "local" estimates of the potential over the range of energies being fitted. Hence, the outer tail of the potential may be approximated by the results of a series of piecewise fits. Further-

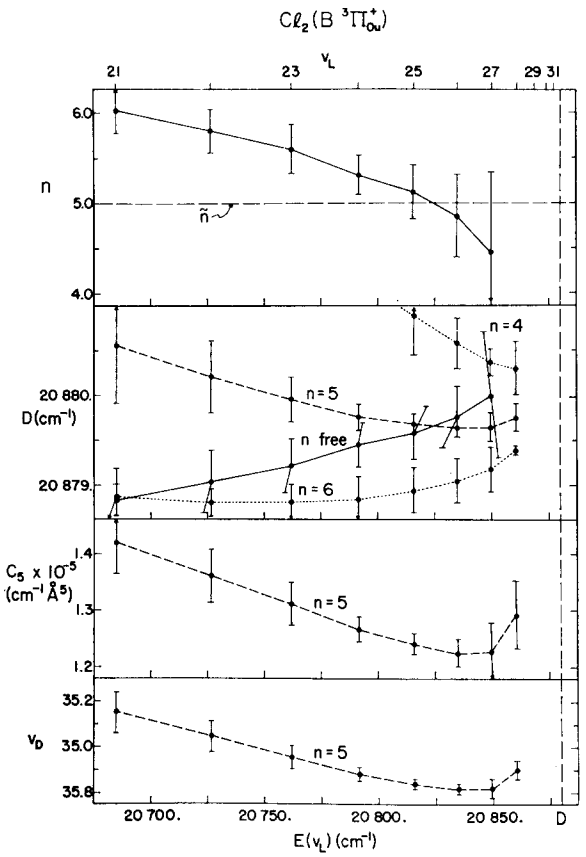

FIG. 5. Results of fitting Eq. (6)[26,29] to the experimental vibrational energies of Cl_2 ($B\ ^3\Pi_{0u}^+$).[36,37] The points correspond to fits of levels v_L up to $v_H=31$. The broken vertical line is the best estimate obtained for D. Points joined by solid curves correspond to four-parameter fits with n varied freely, while the others correspond to three-parameter fits with n held fixed at the indicated values.

more, since all of the pieces should correspond to the same value of D, holding D fixed at the "best" value obtained above should improve the accuracy of the derived potential, particularly for the deeper segments. To explore this point, levels v_L to v_H were fitted to Eq. (6),[29] with D held fixed at 1.0 and $v_H-v_L=4$, while v_H was successively decreased from 23 to 17. The resultant "local" curves are shown in Fig. 4 (only the segments corresponding to odd v_H have been included); the points are the exact turning points, and in this region are indistinguishable from the $-2/R^6$ asymptotic tail. As expected, the fitted segments are somewhat too deep. However the "nesting" of the successive segments shows the decreasing error in the fitted n and C_n as the dissociation limit is approached.[23]

B. Dissociation Limit and Potential Tail of $Cl_2(B\ ^3\Pi_{0u}^+)$

The method is now applied to experimental data for the $B\ ^3\Pi_{0u}^+$ state of Cl_2. Douglas, Møller, and Stoicheff[36] have reported accurate vibrational energies of levels $v=6$ to 31 of this state, the highest observed level lying only a few cm^{-1} below D. A B–S plot of their data shows positive curvature above $v=11$, and hence, these higher levels may be treated by the present method. In what follows, the zero of energy is conveniently set at the lowest vibrational–rotational level of the ground ($X\ ^1\Sigma_g^+$) electronic state; results are reported in the conventional spectroscopic energy and length units: cm^{-1} and angstroms.[37]

As in the LJ (12,6) case, the vibrational energies[36] were repeatedly fitted to Eq. (6) (with four free parameters)[26,29,33] while the deeper levels were successively omitted from consideration, yielding the values of n shown in Fig. 5. Theory indicates[38] that $\tilde{n}=5$ for this state. The fact that the fitted n falls slightly below 5 (for $v_L=26$ and 27) is probably due to the second type of error discussed in Sec. II.C. Over the region where the fitted $n \lesssim 5$, the eigenvalue distribution is probably dominated by the R^{-5} term in the potential. In view of this, the data were refitted to Eq. (6) with n held fixed at 5,[26,29,33] to yield the estimates of D, C_n, and v_D joined by the dashed lines in Fig. 5. These ($n=5$) values of D are also compared to those obtained from analogous fits with n fixed, respectively, at 4 and 6 (dotted curves). A comparison of the limiting $[E(v_L)\rightarrow D]$ behavior of the three D curves for fixed n supports the conclusion that the highest five or six levels lie in the asymptotic $\tilde{n}=5$ region. Furthermore, comparison of the $n=5$ and "n free" curves suggests that the former gives the more reliable estimate of D. This determination of $\tilde{n}=5$ for this state (in agreement with theory) differs with the conclusion of Byrne, Richards, and Horsley[39]; the source of the error in the earlier work is discussed in Ref. 30.

The present analysis yields $D=20\,879.75(\pm 0.15)$ cm^{-1}, $C_5=1.29(\pm 0.06)\times 10^5$ cm^{-1} Å^5, and $v_D(n=5)=34.90(\pm 0.04)$.[40] This value of D is in agreement with, but is considerably more precise than the experimenters' best estimate[36] of $D=20\,880(\pm 2.0)$ cm^{-1}. The above C_5 compares well with the theoretical value[41] of $1.4_4\times 10^5$ cm^{-1} Å^5. Furthermore, the fitted value of v_D implies that there exist at least three unobserved bound levels above $v=31$. Table I lists the predicted level energies, obtained by substituting $n=5$ and the above values for the other three constants into Eq. (6).

It is interesting to explore the question of the accuracy of the D value which would have been obtained by the present method if the data for a few of the highest observed levels had not been available. In this case, the effective local potential for the highest remain-

TABLE I. Calculated energies (in cm^{-1}) for unobserved bound $Cl_2(B\ ^3\Pi_{0u}^+)$ levels.[37]

v	32	33	34
$E(v)$	20878.69	20879.49	20879.73

ing levels would not be dominated by the asymptotic R^{-5} term, so general four-parameter fits to Eq. (6) are necessary (cf. the three-parameter, n fixed at $\tilde{n}$ fits described above). Experimental energies were repeatedly fitted to Eq. (6), eight at a time, as the highest observed levels were successively dropped from consideration.[26,29,33] Figure 6 shows the values of D so obtained plotted vs the energy of the highest level included in a given fit $E(v_H)$.[42] It is noted that even if no levels had been observed above $v=20$ (which lies ≈ 244 cm^{-1} below D), the present method would have yielded an estimate of D within 5.5 cm^{-1} of the present "best" value! In contrast, a linear B–S extrapolation from $v=20$ yields an error in D of ≈ 69 cm^{-1}.

To obtain an estimate of the tail of the $Cl_2(B\,^3\Pi_{0u}^+)$ potential curve, the data were again fitted to Eq. (6)[29] eight levels at a time, except this time D was held fixed at the "best" value of 20 879.75 cm^{-1}.[43] In Fig. 7 the segmented potential so obtained is compared to the RKR turning points calculated by Todd, Richards, and Byrne.[44]

IV. CONCLUDING REMARKS

It has been shown that the distribution of vibrational levels near the dissociation limit of a diatomic molecule is governed mainly by the long-range attractive tail of the internuclear potential.[45] A simple approximate analytic expression has been derived for this distribution, in terms of the dissociation limit D, the power n and coefficient C_n of the effective local inverse-power potential, and an integration constant v_D (which has physical significance if $n=\tilde{n}$). These quantities may be determined via a least-squares fit of experimental vibrational energies to this equation.[26,29,33]

This approach yields the binding energy of the highest observed level with an error of at most a few percent, which is far superior to the error often resulting from use of the customary B–S extrapolation procedures.[3]

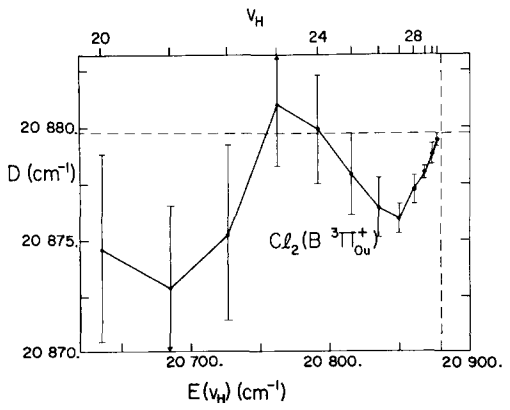

FIG. 6. D estimates obtained by fitting Eq. (6) to the energies of levels v_L to v_H,[26,29] where $v_H - v_L = 7$ and v_H is varied. The vertical and horizontal broken lines denote the best present estimate of D.

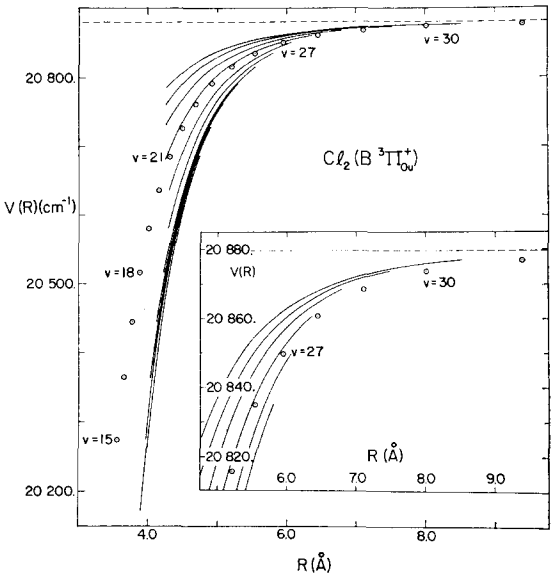

FIG. 7. Piecewise potentials constructed from three-parameter fits (with the constraint $D=20\,879.75$ cm^{-1}) of the experimental vibrational energies[36] of $Cl_2(B\,^3\Pi_{0u}^+)$ to Eq. (6).[26,29] ⊙, RKR turning points for the specified levels[44]; —, segments obtained from fits.

It also leads to a determination of the power n and coefficient C_n of the asymptotically dominating lowest-power term in the inverse-power expansion for the potential; the results for $Cl_2(B\,^3\Pi_{0u}^+)$ accord well with theory.[46] In addition, one obtains an estimate of the outer branch of the potential over the range of the highest levels, albeit less accurate than that obtainable from an RKR potential.[7] However, the present method is much less restrictive in its data requirements and hence, may be applied in many situations where the RKR approach cannot. Here the only restrictions on the input data are that the levels must lie near the dissociation limit D, and that their B–S plot show positive curvature.[47]

A useful additional feature of the present method is its ability (when $n=\tilde{n}$) to predict the energies of all unobserved levels lying above the highest observed level.

The main alternative methods of obtaining estimates of D from spectroscopic data are through use of the less accurate B–S extrapolation (referred to earlier) or from the limiting curve of dissociation (LCD).[3,4] In the latter case, D is deduced by extrapolation to zero J of plots of the uppermost observed rotational levels vs $J(J+1)$. A large uncertainty in D is introduced by the problem of determining the breaking-off point $J_{\max}$ for each v; this is particularly important for the vibrational levels predissociating at small J, closest to the intercept of the LCD at D [e.g., see the case of $Br_2(B\,^3\Pi_{0u}^+)$ discussed in Ref. 30]. It appears that the LCD method is less reliable than the present one.

Alternative spectroscopic approaches to the deter-

mination of $\tilde{n}$ and $C_n(n=\tilde{n})$ are the standard RKR procedure and the predissociation method of Bernstein.[48] Difficulties in the use of the former are discussed in Ref. 30. The latter has been found to yield reasonable results for a number of systems[38,48,49]; however, it suffers from the above-mentioned problem of determining J_{max}. Furthermore, it presupposes an accurate value of D. In general, therefore, $\tilde{n}$ and $C_n(n=\tilde{n})$ values extracted from predissociation data are expected to be less reliable than those obtainable by the present method.

In addition to spectroscopic methods, atomic beam scattering measurements yield $\tilde{n}$ and $C_n(n=\tilde{n})$ values of roughly the same accuracy as those obtained from the present method.[50] These two techniques are essentially complementary. The present approach is best applied to electronic states of a strongly ("chemically") bound molecule with many vibrational levels, where the profusion of electronic states arising from the interaction of all but closed-shell atoms precludes the use of scattering measurements. On the other hand, the shallow van der Waals potential wells normally encountered with closed-shell atoms, ideal for study by the beam scattering technique, do not support enough bound states to be treated by the present method.

The new approach has been demonstrated by applying it to the exact computed eigenvalues of a model LJ (12,6) potential, and to the accurate experimental vibrational energies of $Cl_2(B\,^3\Pi_{0u}^+)$. In companion papers,[30] it is applied to the ground ($X\,^1\Sigma_g^+$) state of Cl_2 and to the $B\,^3\Pi_{0u}^+$ states of Br_2 and I_2, and appears to be of quite general utility.[51] In addition, arguments based on it greatly facilitated the electronic reassignment of some levels of I_2 (see the reference cited in Ref. 21).

ACKNOWLEDGMENTS

The authors appreciate some relevant comments on interatomic forces by Professor J. O. Hirschfelder. They also acknowledge some early correspondence between R. B. B. and Dr. C. L. Beckel and discussions with Dr. H. Harrison, which helped pave the way for the present approach.

APPENDIX A: BIRGE–SPONER PLOTS FOR DIFFERENT POTENTIALS WITH IDENTICAL LONG-RANGE TAILS

The basis of the present method is the conclusion [Eq. (4)] that near the dissociation limit D, the density of vibrational levels $dv/dE(v)$ is determined almost solely by the nature of the outer (attractive) branch of the potential. Thus, B–S plots of the level spacings for different potentials with identical long-range tails and the same reduced mass (but with arbitrarily different short-range behavior) will be identical near the dissociation limit, provided their abscissa (v) scales are shifted appropriately relative to one another. This may be tested either by using exact (quantal) eigenvalues for suitably chosen potentials or, with little loss in accuracy, by the use of WKB-approximated eigenvalues. The latter procedure has been employed here. Reduced WKB integral tables are available for LJ (12,6) and exp(α, 6) ($\alpha=12.0$, 13.772, and 15.0) potentials.[6,52] The LJ (12,6) potential considered in these comparisons[8] is that utilized in Sec. III.A; throughout the present Appendix, all energies and lengths are scaled relative to its well depth and equilibrium distance, and the reduced mass μ is assumed to be the same.

For an exp(α, 6) potential with the same long-range R^{-6} tail as the model LJ (12,6),[8]

$$C_6=2=\frac{D_eR_e^6}{(1-6/\alpha)}. \tag{A1}$$

For any choice of D_e, Eq. (A1) defines the corresponding R_e; the appropriate B_z value[6] is then obtained by multiplying the $B_z(=10\,000.)$ for the model LJ (12,6) potential[8] by $D_eR_e^2$. The parameters of the chosen exp(α, 6) potentials are given in Table AI.

For LJ (12,6) and exp(α, 6) potentials with $\alpha=12.0$, 13.772, and 15.0, the WKB integral tables[6,52] [based on a reduced form of Eq. (1)] are presented as values of $\phi=(v+\frac{1}{2})/B_z^{1/2}$ vs $K\equiv-[D-E(v)]/D_e$ and $\theta\equiv(J+\frac{1}{2})^2/B_z$. Thus[5]

$$\Delta G(v)=(D_e/B_z^{1/2})\,dK/d\phi. \tag{A2}$$

Ignoring the Langer correction[16] for rotationless levels (i.e., using ϕ values for $\theta=0$, rather than for $J=0$),[53] one may obtain $dK/d\phi$ by direct numerical interpolation.[54] $\Delta G(v)$ values thus obtained, via Eq. (A2), yield curves B, C, D, and E in Fig. 8. The points on curve D are the exact quantal[8] vibrational spacings for this case,[5] $\Delta G_{v+1/2}$. Case A refers to a purely attractive potential $V(R)=D-2/R^6$, and Curve A was generated by substituting Eq. (6) into Eq. (4), with $n=6$ and $C_6=2$.[55] The abscissa scales have been shifted to make all v_D's coincide. The insert on Fig. 8 shows the five potentials of the same C_6.

The convergence of the different curves in Fig. 8 as the dissociation limit is approached is considered good evidence of the practical validity of the present method. Increases in reduced mass μ and/or the depth or breadth of the potentials (introducing more vibrational levels) would merely stretch the ordinate and abscissa scales and shift the lower curves up towards Curve A (which would remain unchanged).

TABLE AI. Parameters of exp(α, 6) potentials having same long-range tail as the model LJ (12,6).[8]

Case	E	C	B
α	12.0	13.772	15.0
D_e	1.0	1.5	2.0
R_e	1.0	0.953701	0.918386
B_z	10 000.0	13 643.20	16 868.65

APPENDIX B: ASYMPTOTIC INVERSE-POWER $\tilde{n}$ FOR ATOMIC INTERACTIONS

This section summarizes rules for determining the limiting asymptotic power $\tilde{n}$ in the internuclear interaction. It is based on the references cited in Refs. 20, 41, 56, and 57, and is limited to first- and second-order perturbation theory results. Magnetic (or relativistic) effects are ignored; this is reasonable for $R \lesssim 20$ a.u.,[58] and levels with outer turning points at larger distances would not be readily observed.

The $\tilde{n}$ of the lowest-order term in the inverse-power series expansion [Eq. (13)] for the long-range internuclear potential is determined by the nature of the two atoms to which the molecular state adiabatically dissociates. If the two atoms are charged, of course $\tilde{n}=1$; if one is charged and the other is in an electronic state with a permanent dipole moment,[59] $\tilde{n}=2$; if both atoms are uncharged and in electronic states with permanent dipole moments,[59] $\tilde{n}=3$. Another case in which $\tilde{n}=3$ occurs is in the interaction between two identical uncharged atoms in electronic states whose total angular momenta differ by one (i.e., $\Delta L=1$). This interaction is a first-order dipole resonance[56] and unlike the effects mentioned above, has no classical electrostatic analog. For interactions between a charged and a neutral atom, $\tilde{n}=4$ and $C_4=\frac{1}{2}(Z^2e^2\alpha)$, where Ze is the charge on the ion, and α the polarizability of the neutral. The case $\tilde{n}=4$ can also arise in the interaction of an atom with a permanent electric dipole moment,[59] and a non-S-state atom with a permanent quadrupole moment.

In general, pairs of (uncharged) non-S-state atoms have a first-order quadrupole–quadrupole interaction which corresponds to $\tilde{n}=5$, and theoretical C_5 values are available for a wide range of systems.[41] Occasionally the C_5 coefficient for a particular state is zero for reasons of symmetry [e.g., for the ground $(X\,^1\Sigma_g^+)$ state of the halogens[38]], and in this case $\tilde{n}=6$. For states which do not fall into any of the above classifications, $\tilde{n}=6$ (since all interacting species are subject to the London induced dipole–induced dipole forces).

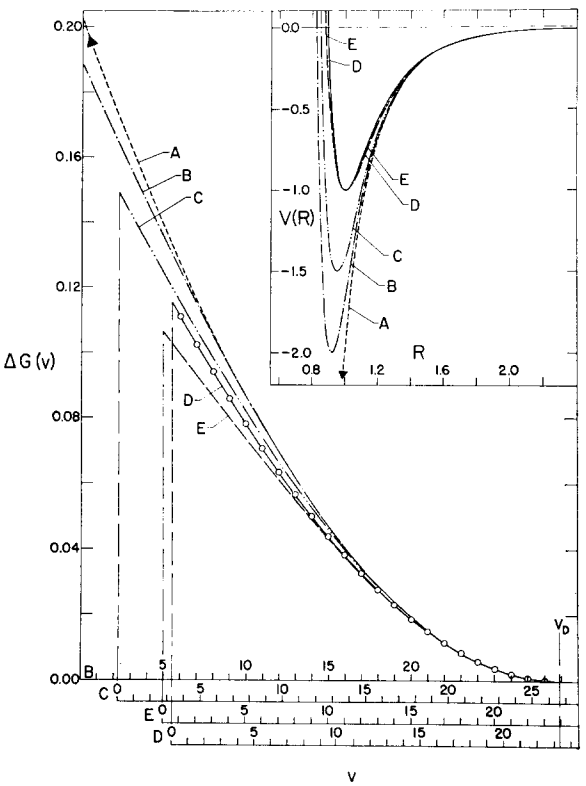

FIG. 8. Birge–Sponer plots for various potentials [LJ (12,6), $\exp(\alpha, 6)$ and pure R^{-6}] with the same long-range tail; the insert shows the corresponding potential curves. A: pure R^{-6}, $V(R)=D-C_6/R^6$; B, C, and E: $\exp(\alpha, 6)$, see Table AI; D: "model" LJ (12,6).[8] All B–S curves except A were generated from Eq. (A2) using WKB integral tables.[6,52] The points are exact quantal level spacings for the LJ (12,6) case,[8] and they confirm the accuracy of the WKB approximation. Curve A was obtained on substituting Eq. (6) into Eq. (4).[55]

* Work supported by National Science Foundation Grant GP-7409 and National Aeronautics and Space Administration Grant NGL 50-002-001. R. J. L. acknowledges with thanks the award of a National Research Council of Canada Postgraduate Scholarship.

[1] R. T. Birge and H. Sponer, Phys. Rev. **28,** 259 (1926).

[2] R. T. Birge, Trans. Faraday Soc. **25,** 707 (1929).

[3] For a recent review see A. G. Gaydon, *Dissociation Energies* (Chapman and Hall Ltd., London, 1968), 3rd. ed.

[4] G. Herzberg, *Molecular Structure and Molecular Spectra: I. Spectra of Diatomic Molecules* (D. Van Nostrand Co., Inc., Toronto, 1950), 2nd ed.

[5] Note that while $\Delta G(v)$ is Herzberg's ΔG_v, $\Delta G(v+\frac{1}{2}) \equiv dE(v+\frac{1}{2})/dv$ is not identical to the "observable" vibrational level spacing

$$\Delta G_{v+1/2}=\int_v^{v+1} \Delta G(v)\,dv$$

(see p. 98 in Ref. 4).

[6] (a) H. Harrison and R. B. Bernstein, J. Chem. Phys. **38,** 2135 (1963); (b) Erratum **47,** 1884 (1967).

[7] See the review by E. A. Mason and L. Monchick, Advan. Chem. Phys. **12,** 329 (1967).

[8] The parameters of the LJ (12, 6) potential were chosen to allow for 24 bound states. In the notation of Ref. 6, this corresponds to $B_e=2\mu D_e R_e^2/\hbar^2=10\,000$, where D_e is the well depth, and R_e the position of the potential minimum. Eigenvalues were calculated numerically and are accurate to 10^{-7} D_e. This was done using a slightly modified form of the Cooley–Cashion program: J. W. Cooley, Math. Computation **15,** 363 (1961); J. K. Cashion, J. Chem. Phys. **39,** 1872 (1963).

[9] I. S. Gradshteyn and I. M. Ryzhik, *Table of Integrals, Series and Products* (Academic Press Inc., New York, 1965), Sec. 3.251, p. 295.

[10] M. Abramowitz and I. Stegun, Natl. Bur. Std. (U.S.), Appl. Math. Ser. **55** (1964); also *Handbook of Mathematical Functions* (Dover Publications, Inc., New York, 1965).

[11] This is because a direct fit of experimental data to Eq. (4) requires a prior numerical smoothing of the data to obtain accurate values of the derivatives $dE(v)/dv$.

[12] It is interesting to note that for $n=4$ (ion-induced dipole forces) Eq. (6) is simply a quartic in v, and for $n=6$ (induced dipole–induced dipole, London dispersion forces) it is cubic.

[13] By comparing Eq. (1) for $E(v)=D$ and $E(v)$ at a slightly smaller v, W. C. Stwalley (private communication, 1969) independently obtained a result for $n=6$ which, upon generalization for any $n>2$, may be cast into the useful form of Eq. (6). However, his factor equivalent to the present K_n is slightly less general, and his approach (unlike the present one) cannot be applied to cases with $n\leq 2$. While seeking a "natural" analytic expression to describe the vibrational spectrum of H_2, C. L. Beckel [J. Chem. Phys. **39,** 90 (1963)] proposed empirical formulas somewhat similar in form to Eq. (6).

[14] P. M. Morse and H. Feshbach, *Methods of Theoretical Physics* (McGraw-Hill Book Co., New York, 1953), Vol. 2, Sec. 12.3.

[15] For pure inverse-power potentials with $n>2$, there are a finite number of levels within any finite neighborhood of the dissociation limit, but there are an infinite number of discrete levels below it, extending down to infinite binding energy. For potentials with $n<2$, there exists a lowest level bound by a finite energy, while there are an infinite number of levels within any finite neighborhood of D. For $n=2$, the levels extend down to infinite binding energy, and there are an infinite number of levels in any finite neighborhood of D.

[16] R. E. Langer, Phys. Rev. **51,** 669 (1937). Using the Langer WKB modification [i.e., replacing $J(J+1)$ by $(J+\frac{1}{2})^2$] would require replacing Eq. (3a) by

$$V(R)=D-(C_n/R^n)+(\hbar^2/2\mu)(1/4R^2).$$

For $n=2$ this just means that C_2 in Eq. (7) becomes $[C_2-(\hbar^2/8\mu)]$, but for $n\neq 2$, the integral arising from Eq. (2) is no longer analytically soluble. However, for realistic systems the Langer correction is fortunately very small.

[17] Within the context of the present approach, potentials with exponential long-range tails (such as the Morse potential) correspond qualitatively to inverse-power potentials with very large n. The purely attractive exponential potential has both a discrete lowest level and a finite number of bound states within any finite neighborhood of D.

[18] A linear B–S plot for levels near the dissociation limit of a potential will be considered as an indication that the potential in the given region is effectively exponential in form.

[19] Care should be taken to avoid confusion between the well depth D_e and D, the position of the dissociation limit.

[20] See the discussion of intermolecular forces in (a) J. O. Hirschfelder, C. F. Curtiss, and R. B. Bird, *Molecular Theory of Gases and Liquids* (John Wiley & Sons, Inc., New York, 1964). (b) J. O. Hirschfelder and W. J. Meath, Advan. Chem. Phys. **12,** 3 (1967).

[21] Note that in the case where some of the dominant terms in Eq. (13) are repulsive (i.e., their $C_m<0$), some of these weighting factors will have differing signs, and the resulting value of n may then lie outside the range of the m's of the contributing terms. If the lowest inverse-power term is repulsive while the higher power terms are attractive, this gives rise to a potential maximum at large R. This appears to be the case for the $^3\Pi_{0g}^+$ state of I_2; R. J. LeRoy, J. Chem. Phys. **52,** 2678 (1970).

[22] In this context a potential is "well behaved" if it has no potential maximum and no nonadiabatic perturbation.

[23] Of course, both errors approach zero for levels approaching D.

[24] (a) See, e.g., the discussion by J. K. Cashion, J. Chem. Phys. **48,** 94 (1968); see also Appendix A. (b) A. S. Dickinson (private communication, 1968).

[25] See Appendix B for a summary of the theoretical $\tilde{n}$ values for a wide variety of cases.

[26] Nonlinear least-squares regression computer programs for fitting arbitrary analytic functions are available at most computing centers. The present calculations used the University of Wisconsin Computing Center subroutine GASAUS for such fits.

[27] Primes denote differentiation with respect to v; e.g., $E'(v)=dE(v)/dv$.

[28] Parameter values obtained from Eqs. (15) and (16) should, in principle, be just as reliable as those obtained from Eq. (6). However, the former approach requires a prior smoothing of the data to obtain accurate values of the derivatives $E'(v)$ and $E''(v)$,[27] and in practice this introduces some error. Experience has shown that while trial parameter values from Eqs. (15) and (16) are satisfactory, they are measurably improved by four-parameter fittings to Eq. (6).[26]

[29] In all of the results presented, an initial fit of the data to Eqs. (15) and (16) yielded trial parameter values which were used to initiate the general nonlinear fit to Eq. (6).[26,30]

[30] R. J. LeRoy and R. B. Bernstein, (a) Wisc. Theoret. Chem. Inst. Tech. Rept. WIS-TCI-369, 1970. The report contains in an appendix FORTRAN listings of the programs used for carrying out fits to Eq. (6), (15), and (16). (b) See also, "Dissociation Energies of Diatomic Molecules from Vibrational Spacings of Higher Levels: Applications to the Halogens," Chem. Phys. Letters (to be published).

[31] This is mainly because of the problem of averaging the estimates of D and K_n obtained at different values of v, to yield a mutually consistent set of parameters. It is interesting that analogous to Eq. (17)

$$n=[4[E''(v)]^2/E'(v)E'''(v)]-2,$$

but because of the above problem, this expression is less reliable than is Eq. (15).

[32] Since the derivatives are obtained from the highest 11 energies only, they cannot be accurate at the end points, so only the 9 points shown on Fig. 2 are reliable.

[33] Since the input data (level energies) are never completely error free, a given fit should always utilize at least one level more than the number of free parameters being fitted. If there is significant experimental uncertainty in the energies (e.g., more than a few percent of the level spacings), a redundancy of more than one level may be required to yield meaningful values of the parameters.

[34] In the application of this method to the $B\,^3\Pi_{0u}^+$ state of I_2,[30] the experimental uncertainty introduces considerable imprecision into the four-parameter fits, so that n could not be directly determined within required accuracy of better than ± 1.

[35] D. E. Stogryn and J. O. Hirschfelder, J. Chem. Phys. **31,** 1531 (1959). These authors derived an analytic expression [their Eq. (89)] for the exact first-order WKB value of v_D (which omits the effect of the Langer correction[16]). A more exact value of the numerical constant in their Eq. (92) is 1.6826.

[36] A. E. Douglas, Chr. Kn. Møller, and B. P. Stoicheff, Can. J. Phys. **41,** 1174 (1963).

[37] The experimental data for this system are for the most common isotope $^{35,35}Cl_2$; all energies are expressed relative to the $v''=0$, $J''=0$ level of its ground electronic state.

[38] T. Y. Chang, Mol. Phys. **13,** 487 (1967); see also the discussion in Appendix B.

[39] M. A. Byrne, W. G. Richards, and J. A. Horsley, Mol. Phys. **12,** 273 (1967).

[40] In choosing these values it is assumed that the "hook" at the end of the $n=5$ curves in Fig. 5 is significant, illustrating the decrease of the error term for levels farther into the asymptotic ($n=\tilde{n}$) region. The indicated uncertainties (including the error bars in Figs. 5 and 6) correspond to a statistical confidence limit of 95%.

[41] It has been shown by J. K. Knipp [Phys. Rev. **53,** 734 (1938)] that C_5 coefficients may be expressed as a product of an angular factor and $[\langle r_A^2\rangle\langle r_B^2\rangle]$, the product of the expectation values for the square of the electron radii in the unfilled valence shells on interacting atoms A and B. Knipp presented values of the angular factors and approximate expectation values for a few systems, and T. Y. Chang [Rev. Mod. Phys. **39,** 911 (1967)] extended these results considerably. Recently C. F. Fischer [Can. J. Phys. **46,** 2336 (1968)] has reported Hartree–Fock values of $\langle r^2\rangle$ for all shells of atoms from He to Rn.

[42] The erratic nature of the curve in Fig. 6 is due to the influence of small errors in the experimental energies on the fitted values of the parameters; the corresponding values of n, C_n, and v_D show similar behavior. Including more levels in each fit dampens these oscillations.

[43] Holding D fixed dampens the "noise" due to experimental uncertainty,[42] yielding a more reliable segmented potential.

[44] J. A. C. Todd, W. G. Richards, and M. A. Byrne, Trans. Faraday Soc. **63,** 2081 (1967).

[45] For a related discussion of the quasibound states, see A. S. Dickinson and R. B. Bernstein, "Some Properties of Bound and Quasibound States for Various Interatomic Potential Functions," Mol. Phys. (to be published).

[46] While the present method is expected to give values of C_n which are slightly small (see Sec. II.C), there is reason to suspect that the theoretical C_5 value used for comparison[41] may be somewhat too large. M. T. Marron (private communication, 1969) points out that Fischer's[41] values of $\langle r^2\rangle$ are based on Hartree–Fock wavefunctions which do not have correct asymptotic tails and that correcting for this may decrease $\langle r^2\rangle$, and hence the theoretical C_5.

[47] For a few systems, such as isotopic hydrogen and most hydrides, the inverse-power long-range forces are relatively weak, so that the B–S plot shows negative or zero curvature even for the very highest levels.

[48] R. B. Bernstein, Phys. Rev. Letters **16,** 385 (1966).

[49] J. A. Horsley and W. G. Richards. J. Chim. Phys. **66,** 41 (1969).

[50] See, for example, H. Pauly and J. P. Toennies, in *Atomic and Electron Physics: Atomic Interactions, Part A*, L. Marton, B.

Bederson, and W. L. Fite, Eds. (Academic Press Inc., New York, 1968), Vol. 7, Chap. 3.1, p. 227.

[51] Although all of the cases thus far considered correspond to $\tilde{n}=5$ or 6, the present method should be even more successful for systems with smaller $\tilde{n}$ (e.g., $\tilde{n}=4$, for molecules which dissociate to ion+neutral) because of the relatively higher density of levels near D.

[52] The present work utilized the corrected tables reported in Ref. 6b. These are available as Document No. 9499 in the ADI Auxiliary Publications Project, Photoduplication Service, Library of Congress, Washington, D.C. 20540.

[53] Comparison of the ϕ values[6,52] for $\theta=0$ and $\theta=10^{-4}$ shows that this introduces negligible error.

[54] This was done by piecewise fitting of third-order polynomials in ϕ. Despite the rather large gaps between the tabulated points for large ϕ, this is expected to be fairly accurate since the eigenvalue distribution for the highest levels of an R^{-6}-tailed potential is expected to be cubic in v (i.e., in ϕ).[12]

[55] Although the exact v_D is infinite for the pure R^{-6} attractive potential, there are a finite number of levels within any finite interval about D.[15] Hence the quantities (v_D-v) and Curve A in Fig. 8 are significant in the semiclassical (WKB) approximation.

[56] G. W. King and J. H. Van Vleck, Phys. Rev. **55,** 1165 (1939).

[57] H. Margenau, Rev. Mod. Phys. **11,** 1 (1939).

[58] This conclusion is partly based on Chang's conclusion[41] that for the 0_g^+ states of O_2 and Cu_2, these effects do not dominate the interaction until $R>60$ a.u.

[59] This case is, however, relatively uncommon; Hirschfelder and Meath[20b] point out that only an excited H atom can have a permanent dipole moment.

THE JOURNAL OF CHEMICAL PHYSICS VOLUME 52, NUMBER 8 15 APRIL 1970

Dynamic Model for Locally Stiff Ring and Straight Chain Polymers

ELIOT SIMON*
The Rockefeller University, New York, New York 10021

(Received 17 September 1969)

The Rouse–Bueche bead–spring model for high polymers is extended to account for stiffness arising from local torsional and bending interactions. A mechanical model including second- and third-nearest-neighbor bead–spring interactions is developed. The effect of local stiffness is introduced into the normal-mode eigenvalue spectrum via second- and third-nearest-neighbor Hooke's law spring constants. A calculation is made of the effect of stiffness on both the free-draining and hydrodynamic interaction properties of linear and circular high polymers. Experiments for supercoiled circular DNA where local stiffness is expected to be large and circular DNA are compared with theory. The effect of local stiffness is sufficient to account for the differences in intrinsic viscosity between the two species.

I. INTRODUCTION

The well-known Rouse[1]–Bueche[2] bead–spring model for a macromolecule has been extended to account for excluded volume[3] and internal viscosity,[4] both of which are expected for more realistic treatments of high polymers. The extensions are of particular interest for deoxyribonucleic acid (DNA) which has been shown through hydrodynamic measurements[5–7] and electron microscopy[8] to exist in the circular as well as linear forms. A characteristic feature of the extensions of the RB model is the change in the eigenvalue spectrum of the normal modes of motion. The treatment of Cerf,[4] for example, takes internal structure into account via frictional forces due to intramolecular torques, which may arise in the presence of a shear gradient. Bloomfield and Zimm[3] have considered the perturbation from Gaussian statistics expected for stiffness and excluded volume due to the hydrodynamic, solvent-mediated interaction. Both effects are put in a term ϵ, which appears in a modified eigenvalue spectrum. Van Beek and Hermans[9] have included internal viscosity effects and found a modified eigenvalue spectrum. Reinhold and Peterlin[10] included modifications for flow properties in a modified, nearest-neighbor spring matrix.

Alternant approaches to polymer dynamics have been suggested recently. The models of Harris and Hearst,[11] Saito *et al.*,[12] and Bugl and Fujita[13] use a continuous representation of the polymer backbone in the form of a stiff wire. A variational calculation using Hamilton's principle is used to derive an equation of motion for the wire. The results show the dynamics of a high polymer, which is expected to be more realistic than the statistical bead–spring model in which bending and torsional motion is not adequately treated.

The present work is an extension of the RB model to include local stiffness expected for DNA, for example. The model makes use of nearest-neighbor bead–spring interactions. The bending and torsional motion is restricted by including two additional Hooke's law spring constants for the second- and third-nearest-neighbor beads. A calculation is made as to the effect of the additional springs on both the free-draining and hydrodynamic behavior via the eigenvalues of the normal mode problem. The results show the effect of the added springs on the relaxation time spectrum.

II. MODEL

The model of $N+1$ beads connected by N springs in a linear fashion developed by Beuche[2] and Rouse[1] and extended by Zimm[14] for the case of hydrodynamic interaction will be used as a starting point for the development. The model considers the $N+1$ beads labeled 0, 1, 2, $\cdots$, j, $\cdots$, N to be governed by Brownian forces, viscous retarding forces, and springlike